

University of Groningen

The pharmacodynamic effects of a dopamine-somatostatin chimera agonist on the cardiovascular system

Joost van Esdonk, Michiel; Stevens, Jasper; Stuurman, Frederik E; de Boon, Wadim M I; Dehez, Marion; Hein van der Graaf, Piet; Burggraaf, Jacobus

Published in:
Journal of Cardiovascular Pharmacology

DOI:
[10.1097/FJC.0000000000000695](https://doi.org/10.1097/FJC.0000000000000695)

IMPORTANT NOTE: You are advised to consult the publisher's version (publisher's PDF) if you wish to cite from it. Please check the document version below.

Document Version
Publisher's PDF, also known as Version of record

Publication date:
2019

[Link to publication in University of Groningen/UMCG research database](#)

Citation for published version (APA):

Joost van Esdonk, M., Stevens, J., Stuurman, F. E., de Boon, W. M. I., Dehez, M., Hein van der Graaf, P., & Burggraaf, J. (2019). The pharmacodynamic effects of a dopamine-somatostatin chimera agonist on the cardiovascular system. *Journal of Cardiovascular Pharmacology*, 74(2), 128-136. <https://doi.org/10.1097/FJC.0000000000000695>

Copyright

Other than for strictly personal use, it is not permitted to download or to forward/distribute the text or part of it without the consent of the author(s) and/or copyright holder(s), unless the work is under an open content license (like Creative Commons).

The publication may also be distributed here under the terms of Article 25fa of the Dutch Copyright Act, indicated by the "Taverne" license. More information can be found on the University of Groningen website: <https://www.rug.nl/library/open-access/self-archiving-pure/taverne-amendment>.

Take-down policy

If you believe that this document breaches copyright please contact us providing details, and we will remove access to the work immediately and investigate your claim.

Downloaded from the University of Groningen/UMCG research database (Pure): <http://www.rug.nl/research/portal>. For technical reasons the number of authors shown on this cover page is limited to 10 maximum.

The pharmacodynamic effects of a dopamine-somatostatin chimera agonist on the cardiovascular system

Michiel Joost van Esdonk, MSc^{1,2}, Jasper Stevens, Dr³, Frederik E. Stuurman, MD², Wadim M.I. de Boon, MD², Marion Dehez, Dr⁴, Piet Hein van der Graaf, Prof^{1,5}, Jacobus Burggraaf, Prof^{1,2}

Affiliations:

¹Division of Systems Biomedicine and Pharmacology, Leiden Academic Centre for Drug Research, Leiden University, Leiden, The Netherlands.

² Centre for Human Drug Research, Leiden, The Netherlands.

³ Department of Clinical Pharmacy and Pharmacology, University of Groningen, University Medical Center Groningen, Groningen, Netherlands

⁴ Ipsen Innovation, Les Ulis, France.

⁵ Certara QSP, Canterbury, UK.

Corresponding author:

Koos Burggraaf, Centre for Human Drug Research, Zernikedreef 8, 2333 CL Leiden, The Netherlands

Tel: +31 71 524 6400, E-mail: kb@chdr.nl

Running title: PD effects of BIM23B065 on the RPP

EudraCT number = 2014-004561-24

Conflict of interest:

MJVE: None, JS: None, FES: None, WMIDB: None, MD: Employee of Ipsen, PHVDG: None, JB: None. This study was funded by Ipsen.

Abstract

The quantification of the effect of pharmacological treatment on the cardiovascular system is complicated due to the high level of inter-individual and circadian variability. Recently, a dopamine-somatostatin chimera, BIM23B065, was under investigation to concurrently target the somatostatin and dopamine D₂ receptors for the treatment of neuroendocrine tumors. However, both dopamine and somatostatin interact with different components of the cardiovascular system. This study established the response of the heart rate and the systolic blood pressure after administration of BIM23B065 in healthy male volunteers by analysis of the rate-pressure product (RPP), in a model informed analysis.

The RPP in the supine position of placebo treated subjects showed a clear circadian component, best described by two cosine functions. The pharmacokinetics of BIM23B065 and its metabolite were best described using 2-compartment models with different forms of elimination kinetics. The administration of BIM23B065 gave a statistically significant reduction in the RPP, after which the effect diminished due to tolerance to the cardiovascular effects after prolonged exposure to BIM23B065.

This model provided insight in the circadian rhythm of the RPP in the supine position and the level of inter-individual variability in healthy male volunteers. The developed population pharmacokinetic/pharmacodynamic model quantified the interaction between BIM23B065 and the RPP, informing on the clinical pharmacological properties of BIM23B065.

Keywords: rate-pressure product, neuroendocrine tumors, acromegaly, PK/PD modeling, phase I clinical trial

Introduction

The quantification of the effect of pharmacological treatment on the cardiovascular system is complicated due to the high level of intrinsic biological variability in this system, which include circadian rhythmicity and interacting feedback components (1). This biological information is neglected when a dose-response analysis is performed, directly linking the administered dose to the observed outcome. These analyses do not take into account the individual exposure to a drug, the concentration-effect relationship, or the difference in response after multiple dosing, causing a discrepancy in the quantification of the true relationship between physiology and pharmacology. More information can be obtained on the response of a biological system after pharmacological intervention by the use of population non-linear mixed effects models (2).

Recently, a novel class of compounds, dopastatins, were under investigation for the treatment of neuroendocrine tumors. Dopastatins are dopamine-somatostatin chimera compounds, covalently linking a somatostatin analog with a dopamine analog (3). They are anticipated to improve the efficacy of growth hormone inhibition by concurrently targeting both the somatostatin (ssr_2 and ssr_5) and dopamine D_2 receptors, expressed on pituitary adenomas (3–5). However, the molecular

targets of a dopastatin are also interacting with the cardiovascular system. Treatment with dopamine agonists are known to cause a decrease in blood pressure (6–8), whereas treatment with somatostatin analogs cause a significant drop in heart rate by binding to receptors in the vagus nerve (9).

A first generation dopastatin gave promising *in vitro*, *in vivo* and clinical results but development was halted due to the formation of an active interfering metabolite (3). A second generation dopastatin, BIM23B065, was under development and was recently investigated in a phase 1 clinical trial in healthy male volunteers (10). This second generation compound showed promising endogenous and stimulated growth hormone lowering properties at subcutaneous (s.c.) doses upwards of 0.4 mg (10). BIM23B065 was not excreted in the urine and an interspecies *in vitro* metabolite profiling study showed that BIM23B065 was primarily metabolized by the S9 fraction from the kidney, pancreas and small intestine, resulting in the formation of the main metabolite (BIM23B133). This metabolite was primarily cleared by the kidney and showed weak D₂/sst efficacy and no interference with the effects of BIM23B065 *in vitro* (11).

In this phase 1 clinical trial, cardiovascular effects of treatment with BIM23B065 were identified (10). During treatment with BIM23B065, orthostatic hypotension (n = 8; 28% of BIM23B065 treated subjects) or syncope (n = 1; 3%) was reported during the single ascending dose part of the study. To counter these effects, an up-titration period was included in the multiple ascending dose part of the study where orthostatic hypotension still occurred in a high percentage of BIM23B065 treated subjects (n = 20; 83%) but no syncope was reported and side effects were less prominent (10). These results suggested that there was a reduction in the severity of symptomatic cardiovascular events after an up-titration period, but questions remained unanswered on the level of inter-individual variability in the response, the variability in tolerance to the dopaminergic

effects after multiple dosing, the simultaneous interaction with the different cardiovascular outcomes and the pharmacokinetic/pharmacodynamic (PK/PD) relationship of BIM23B065.

To establish the response of the cardiovascular system after co-targeting of the D₂ and sst receptors, a model informed population PK/PD analysis of BIM23B065 was performed. As such, the heart rate (HR), systolic blood pressure (SBP) and the rate-pressure product (RPP), a marker for myocardial oxygen demand (Equation 1) (12), in the supine position were investigated as pharmacodynamic outcomes.

$$\text{Rate-pressure product} = \text{heart rate (BPM)} \cdot \text{systolic blood pressure (mmHg)}$$

(1)

The effects of BIM23B065 were studied and a concentration-effect relationship was established, while accounting for the circadian rhythm and the inter-individual variability in the response, including the investigation of tolerance to the cardiovascular effects after multiple dosing.

Methods

Trial information

The main clinical trial results have been previously reported in full (10) and the design and methods are summarized in short here. Approval from a medical review and ethics committee (BEBO, Assen, the Netherlands) was obtained and all volunteers signed an informed consent form. This phase 1 clinical trial was performed in a total of 63 healthy young male volunteers and consisted of a single and multiple ascending dose part. The cohorts consisted of 8 planned subjects of which 2 received a placebo and 6 received BIM23B065. One subject withdrew

consent before dosing and was not replaced. BIM23B065 was administered as a 1mL s.c. bolus injection with a rotation of the injection sites in the abdominal region.

Study design

The single ascending dose part of the study consisted of 5 cohorts, receiving doses of 0.1 mg, 0.4 mg, 0.8 mg, 1.2 mg and 1.5 mg. The multiple ascending dose part consisted of 3 cohorts, receiving doses of 1.2 mg q.d., 0.8 mg b.i.d. and 1.0 mg b.i.d.. The b.i.d. doses were administered at an 8h/16h dosing interval. The multiple ascending dose part included a 6 day up-titration period to counteract potential cardiovascular effects of BIM23B065. After this up-titration period, the target dose was given for a total of 7 days, resulting in a total study duration of 13 days.

Pharmacokinetics

The PK samples for BIM23B065 and BIM23B133 were taken in the single ascending dose part and during the final day of dosing of the multiple ascending dose part. Additionally, trough samples were taken at day 7, 11 and 12. PK samples were analyzed using a LC-MS/MS quantification method with a lower limit of quantification (LLOQ) of 0.1 ng/mL. Data below the LLOQ were excluded from model development if it accounted for less than 25% of the total data until 24h after dosing.

Pharmacodynamics

The HR and SBP were measured with a Dinamap V1000 or a Dash 3000 (GE Healthcare) in the supine position after a 10-min resting period. During the single ascending dose part, the HR and SBP were measured pre-dose and at 0.25, 0.5, 1, 2, 3, 4, 6, 8, 12, 24, 48, 72 and 144 hours after

dosing. During the multiple ascending dose part, the HR and SBP were measured pre-dose and at 30 minute intervals up to 4h, 6h, 8h and 12h for the q.d. cohort and every 30 minutes up to 4h post-dose (for each dose) in the b.i.d. cohorts, measurement intervals were reduced in the final 3 dosing days to 0.5h, 1h, 2h, 4h and 8h after q.d. dosing and to 0.5h, 1h, 2h, 4h post-dose (for each dose) in the b.i.d. cohorts.

Data analysis

Structural model development

A sequential non-linear mixed effects (NLME) modeling approach was used in which first the structural model was developed for the PK of BIM23B065, after which the individual post hoc Bayesian parameter estimates were used for the population modeling of BIM23B133 (13). All PK parameters were fixed to their post hoc Bayesian estimates during PD model development. The structural PK model development was focused on the identification of 1-, 2-, or 3-compartment models including first-order, non-linear or a combination of first-order and non-linear elimination kinetics. The s.c. absorption of BIM23B065 was investigated to follow zero- or first-order absorption kinetics. The PK disposition of BIM23B133 was explored using 1-, 2- and 3-compartment models with the use of transit compartments describing a delay of parent to metabolite conversion.

Due to the existing circadian rhythm of HR, SBP and the RPP (14–17), all measurement times were clock time corrected after 6 a.m. A turnover model with a circadian component was developed on the data from placebo treated individuals prior to investigating the effect of

BIM23B065, to prevent bias in the estimation of the circadian rhythm component (2). The circadian rhythm was included using the following equation:

$$k_{in} = \text{mesor} + \text{amplitude} \cdot \cos\left(2\pi \cdot \frac{T - \text{phase shift}}{\text{acrophase}}\right) \quad (2)$$

Where *mesor* is the average input, *amplitude* describes the height of the cosine function and the *phase shift* parameter shifts the start of the period of the cosine function from 6 a.m. The *acrophase* is the time needed for 1 cosine period to be completed. The explored acrophases in this study completed their period in a 24h timeframe, with 6h, 8h, 12h and 24h acrophases tested. The potential influence of a combination of cosine functions was explored by inclusion of an extra cosine function in Equation 2. Consequently, additional *amplitude* and *phase shift* parameters were estimated. Combinations of two cosine functions with an acrophase of 12h or 24h for the first cosine in combination with a 6h, 8h, 12h or 24h acrophase for the second cosine function were explored during model development.

After inclusion of the data from BIM23B065 treated subjects, the concentration-effect relationship was investigated using a linear (Equation 3) or sigmoidal E_{max} (Equation 4) relationship.

$$\text{Effect}(t) = C(t) \cdot \text{Slope} \quad (3)$$

$$\text{Effect}(t) = \frac{E_{max} \cdot C(t)^n}{EC_{50}^n + C(t)^n} \quad (4)$$

Where $C(t)$ is the concentration of the drug over time, *slope* determines the steepness of the concentration-effect relationship, E_{max} is the maximum effect that can be reached, EC_{50} is the concentration at which 50% of the maximum effect is reached and n is the hill coefficient. When the hill coefficient n could not be estimated with adequate precision, it was assumed to be 1. It

was investigated whether the concentrations of BIM23B065, BIM23B133 or the cumulative concentrations of both were driving the effect.

The up-titration period included in the multiple ascending dose part of the study was hypothesized to result in tolerance to the cardiovascular effects over time. Tolerance was investigated in the structural model as a decrease of the *slope*, in the case of a linear PK/PD relationship, or by lowering the E_{max} or increasing the EC_{50} , when an E_{max} relationship was identified, driven by the total exposure over time to BIM23B065.

The random effects (η) were included as a ln-normal distribution, describing the inter-individual variability (IIV) on the population parameters (θ). The η on the phase shift of cosine functions was drawn from a normal distribution. IIV was included in the structural model using a forward inclusion method ($p < 0.05$). For the residual error structure a proportional, additive and a combined (proportional + additive) residual error structure, drawn from a normal distribution, were investigated.

Covariate analysis

The following covariates were explored: age, height, weight, body mass index (BMI) and lean body mass (LBM). LBM was calculated using the Janmahasatian equation (18). Visual and numerical exploration of the individual post hoc random effect estimates versus the covariates, assessing the Pearson correlation, was used for covariate selection. Covariate relationships were judged on biological plausibility. Covariates were included in the structural model as a linear or power relationship and included after a significant ($p < 0.05$) improvement in the model fit. Covariate selection was combined with a backward elimination step ($p < 0.01$).

Model evaluation

Model evaluation was based on the objective function value (OFV), which is $-2 \times \log\text{-likelihood}$, visual inspection of the goodness of fit (GOF) plots, numerical evaluation and internal validation (19,20). Model hypothesis testing was done using the likelihood ratio test under the assumption that it follows a χ^2 distribution. Thus, with 1 additional degree of freedom, a model was statistically improved ($p < 0.05$) if the drop in OFV was more than 3.84 points compared to its parent model. GOF plots were generated visualizing the individual (IPRED) and population (PRED) model predictions versus observations, the conditional weighted residuals with interaction (CWRESI) versus time and PRED, and the individual predicted model fit and observations over time.

Numerical evaluation was based on the uncertainty of population parameters, judged by the relative standard error (RSE) of a parameter, the shrinkage, and the condition number, used to determine proper conditioning of the structural model. The RSE was calculated from the standard error, reported by NONMEM after a successful covariance step (21), divided by the parameter estimate.

A non-parametric bootstrap with 1000 samples was performed to quantify the confidence interval of the population parameter estimates. A visual evaluation of the model was performed by the generation of prediction-corrected visual predictive checks (VPC). VPC's were judged on the ability of the model to capture the median trend and the variability in the data.

Software

Data transformation and graphical analysis was performed in R (V3.5.1) (22). NLME modeling was performed in NONMEM V7.3 (21). NLME modeling was used in conjunction with Perl-speaks-NONMEM V4.4.0 (23).

Results

The demographics of the placebo and BIM23B065 treated subjects were comparable (Table 1). No differences in the subject characteristics between the single and multiple ascending dose cohorts were identified.

Pharmacokinetics

A total of 453 BIM23B065 and 589 BIM23B133 plasma concentrations above the LLOQ were used for PK model development. A total of 19% of BIM23B065 and 3% of the BIM23B133 samples were below the LLOQ in the 24h after dosing, of which the majority originated from the lowest dosing cohorts. The multi-exponential phase after maximal concentration in the PK profiles of BIM23B065 and BIM23B133 (Figure 1) suggested the existence of a peripheral distribution compartment. A 2-compartment model with first-order absorption and combined first-order and non-linear elimination kinetics was able to capture the general trend of the data in both parts of the study best. The residual error structure was best described using a combined (proportional + additive) structure. The forward inclusion of IIV resulted in the identification of significant variability on, in order of inclusion: clearance (CL), absorption rate constant (k_a), and Michaelis-Menten constant (K_M). The inclusion of IIV on the central volume of distribution (V_c).

parent) resulted in a significant drop ($p < 0.05$) in OFV but caused a two-fold increase in the RSE of multiple parameters, and was therefore not included in the model. A significant negative linear covariate relationship between BMI and k_a was identified ($p < 0.001$), possibly due to the increase in hypodermis thickness at higher weights (24).

A 2-compartment model for BIM23B133, originating from both non-linear and first-order metabolization processes of BIM23B065 with a single transit compartment for each process showed to be superior over other tested combinations. First-order elimination of BIM23B133 with a proportional residual error structure was best fit for purpose. Forward inclusion of IIV resulted in the identification of significant variability on CL, the transit rate of the non-linear metabolization process ($KT_{\text{non-linear}}$) and the central volume of distribution ($V_{c\text{-metabolite}}$) of BIM23B133. A binomial distribution was identified in the post hoc Bayesian estimates of BIM23B133 CL. These distributions could be stratified in the single and multiple ascending dose part of the study. When stratified as new population parameters, individuals in the single ascending dose part had a lower CL of BIM23B133 (typical CL = 10.5 L/h, CV = 39%) compared to the multiple ascending dose part (typical CL = 18.5 L/h, CV = 26.2%). No covariates for BIM23B133 were identified.

The parameter estimates of the PK model of BIM23B065 and BIM23B133 are reported in Table 2. The structural PK model is depicted in Figure 2a. The GOF plots (Figure 3a and 3b) indicate adequate individual model predictions, scattered closely around the line of unity. One outlier in the metabolite concentrations was identified (CWRESI of 8+). Exclusion of this sample did not significantly alter the parameter estimates. The CWRESI over the population predictions were homogeneously distributed around 0 with the majority of predictions within the [-2,2] interval, indicating no structural model misspecification in both models. The prediction-corrected VPC's

are depicted in Supplemental 1A/B, <http://links.lww.com/JCVP/A400> which indicate that the median and variability of the data is well described, with a slight overestimation of the variability at the lowest concentrations.

Pharmacodynamics

The exploratory analysis of the BP, SBP and the RPP indicate high variability in the baseline corrected outcomes of placebo and BIM23B065 treated subjects (Figure 4). An initial drop from baseline after dosing can be identified in the placebo subjects, possibly due to the circadian rhythm existing in all outcomes. The HR of placebo subjects is scattered around the baseline level whereas the SBP and RPP show a higher level of variability with decreases below the baseline in the first 12h after dosing. The HR of the five single dose cohorts is similar to the placebo levels, with a continuous mean decrease below baseline in the 1.5 mg cohort. On the last day of dosing (day 13), the HR of the 1.2 mg q.d. and 0.8 mg b.i.d. cohorts were scattered around the baseline. However, the subjects in the 1.0 mg b.i.d. cohort showed a clear reduction in HR, which existed during the full 13 day treatment period.

The SBP of the single ascending dose cohorts up to 0.8 mg show profiles distributed around the baseline, whereas a strong decrease in the SBP ($\Delta\text{SBP} > -10$ mmHg) at the 1.2 and 1.5 mg doses was observed. This decrease was also observed in the 1.2 mg q.d. and 0.8 mg b.i.d. cohorts, whereas the 1.0 mg b.i.d. cohort showed a similar drop in SBP with a rebound up to baseline between the 2 doses.

The RPP is the product of the HR and SBP and therefore combines the information on the response of both outcomes. A similar response with placebo subjects on the RPP at the 0.1 mg and 0.4 mg doses was observed, compared to a longer time to return back to baseline at doses

upwards of 0.4 mg. This indicates that in this healthy population, the compensatory mechanism between HR and SBP was reduced by the dopamine and somatostatin moieties of BIM23B065, resulting in a drop in the RPP. This resulted in a marked mean decrease in the 1.5 mg cohort in the RPP of -1000 bpm*mmHg, even after 12 hours post dose. The decrease in the RPP was less prominent in the 1.2 mg q.d. and 0.8 mg b.i.d. cohorts of the multiple ascending dose part, which suggests a possible tolerance in the RPP in BIM23B065 treated subjects after multiple days of dosing but which is not strong enough to compensate for the decrease in HR in the 1.0 mg b.i.d. cohort. Due to the interaction between HR and SBP in physiology, the effect of BIM23B065 on both the HR and SBP, and this exploratory analysis, the RPP was chosen as the outcome of interest for the development of a PD model on which to quantify the effects of BIM23B065.

The RPP PK/PD model was developed on the data from 16 placebo subjects (1268 RPP measurements) and 47 BIM23B065 treated subjects (3716 RPP measurements). IIV was included on the *mesor* during model building to account for the observed variability in baseline RPP values. The use of a steady-state turnover model, without inclusion of circadian rhythmicity, resulted in a bias in the CWRESI over time (Supplemental 2a, <http://links.lww.com/JCVP/A401>). Further exploration of the RPP resulted in the identification of a circadian rhythm in the data from placebo subjects (Supplemental 3, <http://links.lww.com/JCVP/A402>). This suggests the existence of two bathyphases, dips in the circadian variability, around 12:00 and 20:30, which may explain part of the variability observed in Figure 4. The combination of 2 cosine functions, with 24h and 8h acrophases, was identified as the best structural model describing the circadian rhythmicity with a significant improvement in the model fit and normalization of the CWRESI (Supplemental 2c, <http://links.lww.com/JCVP/A401>).

The inclusion of an E_{max} effect, driven by the PK of BIM23B065 was superior over other tested relationships. Using the PK of BIM23B133 or the cumulative concentrations of BIM23B065 and BIM23B133 as the driving force of the drug effect did not result in a significant improvement. The use of 24h and 8h acrophases combined with an E_{max} concentration-effect relationship gave the largest improvement in model fit ($\Delta OFV = -776$; $p < 0.001$), compared to the exclusion of a drug effect, and was therefore taken forward in model development. Tolerance to the cardiovascular effects of BIM23B065 was identified as a linear effect between the cumulative exposure to BIM23B065 and an increase in the EC_{50} , which reduced the OFV by 33.6 points ($p < 0.001$). IIV was included on the k_{out} , the *phase shift* of the 24h cosine function, the tolerance *slope*, and the *amplitude* of the 24h cosine function with an additive residual error structure. No covariates on the population parameters were identified.

The schematic representation of the PD model for the RPP is depicted in Figure 2b. The parameter estimates of the RPP PK/PD model are presented in Table 3. All drug effect parameters had accurate RSE's ($< 20\%$) but relatively high shrinkage on cosine function parameters (*amplitude* and *phase shift*). The GOF plots show both the IPRED and PRED versus observations and the CWRESI versus PRED for the PD model of placebo subjects (Figure 3c) and BIM23B065 treated subjects (Figure 3d). Model predictions show a homogenous scatter around the line of unity, indicating adequate model predictions. The majority of data points in the CWRESI versus population predictions is between the $[-2, 2]$ interval, with no observable bias present in the data. The prediction-corrected VPC (Supplemental 1C, <http://links.lww.com/JCVP/A400>) indicate that this model is able to fit the median and variability of the data over time of day, taking into account the circadian variability of the RPP. Additional simulations of a typical individual have been performed in which the RPP over time, with dosing

at 10 a.m., is depicted for a placebo subject and the doses administered in the single ascending dose part of the study (Figure 5). This simulation shows the circadian variability in the placebo cohort with the RPP lowering activity of BIM23B065 at increasing doses.

Discussion

The developed PK model was able to fit the observations of BIM23B065 and its metabolite BIM23B133 in both parts of this study. Both the parent and metabolite were best described using 2-compartment structural models with first-order and non-linear elimination kinetics for the parent and first-order elimination for the metabolite. The RPP model was able to capture the circadian rhythm present by the inclusion of two cosine functions, with inter-individual variability on the amplitude of the 24h cosine function, the phase shift, and the turnover rate constant (k_{out}). The established PK/PD relationship shows that BIM23B065 has statistically significant cardiovascular effects by decreasing the RPP, mainly driven by a decrease in the SBP. The identified E_{max} PK/PD relationship was best driven by the concentrations of BIM23B065. No time dependent changes in BIM23B133 clearance were identified, additional PK sampling during the up-titration period will better explain the clearance related changes in metabolite clearance.

The two bathyphases during the day that were estimated in this structural model were also identified by Hermida *et al.*, which used ambulatory monitoring (14). They studied the RPP in a healthy young population using data from a 24 hour cycle. This resulted in the identification of an additional third cosine function for the description of the circadian rhythm of RPP. The collection of data between 10 p.m. and 8 a.m. may inform on this additional cosine function that was not identified in the current study. The inclusion of two cosine functions in the model enabled the

correct description of the variability in the RPP during the day, indicated by the homogenous distribution of the residuals and the distribution in the VPC. However, high shrinkage on multiple components of the model were identified which may be improved by additional data collection at continuous intervals throughout the day.

A decrease in the SBP and HR after dosing with BIM23B065, due to the co-targeting of dopamine and somatostatin receptors, resulted in a significant decrease of the RPP. A decrease in the SBP was already observed in doses upwards of 0.8 mg, which indicates that in these cohorts the drop in RPP is mainly due to SBP effects, which is not compensated for by an increase in the HR. The effect of BIM23B065 on the HR becomes more prominent in the 1.0 mg b.i.d. dose in the multiple ascending dose part, where a clear reduction below baseline was observed. The up-titration period prevented the orthostatic effects in the multiple ascending dose part of the study since side effects were less severe and no syncope was observed. This is supported by the significant increase in the EC_{50} on the RPP, driven by the total exposure to BIM23B065, that was identified on this data. However, there was a high level of IIV on this parameter (CV = 581%) which suggests that the tolerance to the cardiovascular effects of BIM23B065 is highly variable between individuals.

Previously, efficacious growth hormone lowering effects by BIM23B065 were observed after a single dose of 0.8 mg s.c., reaching maximal plasma concentrations of 8.1 ng/mL (10). The estimated EC_{50} of the decrease in RPP (0.24 ng/mL) indicates that at this dose, clear RPP effects are present, although the maximal effect does not seem to be reached (Figure 5). The effect on the RPP after administration of the highest dose administered in this study of 1.5 mg BIM23B065 for a typical individual was a reduction of approximately -1800 mmHg*bpm, compared to placebo (Figure 5). In the exploratory plots of the RPP of the placebo treated subjects (Figure 4) we see a

comparable variability between individuals in which the range was within [-2000, 2000] mmHg*bpm from baseline. This indicates that a significant reduction in the RPP in the highest dosing group (1.5 mg) may not necessarily result in any clinical effects for the typical individual due to its overlap with the placebo distribution. However, a quick decrease in blood pressure and heart rate, combined with the level of variability present in this healthy population, can result in a RPP that is far below this typical value. Therefore, these results confirm the relevance of an up-titration phase to limit the occurrence of these effects, in which the HR and SBP should be closely monitored, when administering BIM23B065.

Conclusion

In conclusion, the circadian rhythm of the RPP was best described with two cosine functions, implementing 24h and 8h acrophases, in healthy male volunteers. A significant reduction in the RPP was quantified after administration of BIM23B065, when corrected for circadian variability. The developed models provided insight in the circadian rhythm of the RPP in the supine position, the level of variability of this outcome in healthy volunteers, and the clinical pharmacological properties of BIM23B065.

Acknowledgment

This study was funded by Ipsen.

References

1. Chen L, Yang G. Recent advances in circadian rhythms in cardiovascular system. *Front Pharmacol* (2015) **6**:71. doi:10.3389/fphar.2015.00071
2. Upton RN, Mould DR. Basic concepts in population modeling, simulation, and model-based drug development: part 3—introduction to pharmacodynamic modeling methods. *CPT Pharmacometrics Syst Pharmacol* (2014) **3**:e88. doi:10.1038/psp.2013.71
3. Culler MD. Somatostatin-dopamine chimeras: A novel approach to treatment of neuroendocrine tumors. *Horm Metab Res* (2011) **43**:854–857. doi:10.1055/s-0031-1287769
4. Hofland LJ, Feelders RA, de Herder WW, Lamberts SWJ. Pituitary tumours: The sst/D2 receptors as molecular targets. *Mol Cell Endocrinol* (2010) **326**:89–98. doi:10.1016/j.mce.2010.04.020
5. Hofland LJ, Lamberts SWJ. Somatostatin receptors in pituitary function, diagnosis and therapy. *Front Horm Res* (2004) **32**:235–52.
6. Nilsson A, Hökfelt B. Effect of the dopamine agonist bromocriptine on blood pressure, catecholamines and renin activity in acromegalics at rest, following exercise and during insulin induced hypoglycemia. *Acta Endocrinol Suppl (Copenh)* (1978) **216**:83–96.
7. Ferrari C, Barbieri C, Caldara R, Mucci M, Codecasa F, Paracchi A, Romano C, Boghen M, Dubini A. Long-Lasting Prolactin-Lowering Effect of Cabergoline, A New Dopamine Agonist, in Hyperprolactinemic Patients. *J Clin Endocrinol Metab* (1986) **63**:
8. Kujawa K, Leurgans S, Raman R, Blasucci L, Goetz CG. Acute orthostatic hypotension

- when starting dopamine agonists in Parkinson's disease. *Arch Neurol* (2000) **57**:1461–1463. doi:10.1001/archneur.57.10.1461
9. Maison P, Tropeano A-I, Macquin-Mavier I, Giustina A, Chanson P. Impact of Somatostatin Analogs on the Heart in Acromegaly: A Metaanalysis. *J Clin Endocrinol Metab* (2007) **92**:1743–1747. doi:10.1210/jc.2006-2547
 10. de Boon WMI, van Esdonk MJ, Stuurman FE, Biermasz NR, Pons L, Paty I, Burggraaf J. A Novel Somatostatin-Dopamine Chimera (BIM23B065) Reduced Growth Hormone Secretion In A First-in-human Clinical Trial. *J Clin Endocrinol Metab* (2018) doi:10.1210/jc.2018-01364
 11. Saveanu A, Datta R, Zhang S, Shen Y, Dong J, Graillon T, Desfilles C, Landsman T, Halem H, Enjalbert A, et al. Novel Somatostatin-Dopamine Chimeric Compound Demonstrates Superior Efficacy in Suppressing Growth Hormone Secretion from Human Acromegalic Tumors Partially Responsive to Current Somatostatin and Dopamine Therapies. *Endocrine's Soc 98th Annu Meet* (2016)
 12. Gobel FL, Norstrom LA, Nelson RR, Jorgensen CR, Wang Y. The rate-pressure product as an index of myocardial oxygen consumption during exercise in patients with angina pectoris. *Circulation* (1978) **57**:549–556. doi:10.1161/01.CIR.57.3.549
 13. Zhang L, Beal SL, Sheiner LB. Simultaneous vs. Sequential Analysis for Population PK/PD Data I: Best-case Performance. *J Pharmacokinet Pharmacodyn* (2003) **30**:387–404. doi:10.1023/B:JOPA.0000012998.04442.1f
 14. Hermida RC, Fernández JR, Ayala DE, Mojón A, Alonso I, Smolensky M. Circadian

Rhythm of Double (Rate-Pressure) Product in Healthy Normotensive Young Subjects.

Chronobiol Int (2001) **18**:475–489. doi:10.1081/CBI-100103970

15. Siegelova J, Fiser B, Dusek J, Placheta Z, Cornelissen G, Halberg F. Circadian variability of rate-pressure product in essential hypertension with enalapril therapy. *Scr Medica* (2000) **73**:67–75.
16. Massin MM, Maeyns K, Withofs N, Ravet F, Gérard P. Circadian rhythm of heart rate and heart rate variability. (2000)179–182.
17. Dehez M, Chenel M, Jochemsen R, Ragot S. Population modeling approach of circadian blood pressure variations using ambulatory monitoring in dippers and non dippers. *PAGE Abstr Annu Meet Popul Approach Gr Eur*
18. Janmahasatian S, Duffull SB, Ash S, Ward LC, Byrne NM, Green B. Quantification of lean bodyweight. *Clin Pharmacokinet* (2005) **44**:1051–65. doi:10.2165/00003088-200544100-00004
19. Nguyen T-H-T, Mouksassi M-S, Holford N, Al-Huniti N, Freedman I, Hooker AC, John J, Karlsson MO, Mould DR, Pérez Ruixo JJ, et al. Model evaluation of continuous data pharmacometric models: Metrics and graphics. *CPT pharmacometrics Syst Pharmacol* (2016) **6**:1–20. doi:10.1002/psp4.12161
20. Bergstrand M, Hooker AC, Wallin JE, Karlsson MO. Prediction-Corrected Visual Predictive Checks for Diagnosing Nonlinear Mixed-Effects Models. *AAPS J* (2011) **13**:143–151. doi:10.1208/s12248-011-9255-z
21. Beal SL, Sheiner LB, Boeckmann AJ, and Bauer RJ (eds) NONMEM 7.3.0 Users Guides.

(1989–2013). ICON Development Solutions, Hanover, MD.

22. R Core Team (2018). R: A language and environment for statistical computing. R Foundation for Statistical Computing, Vienna, Austria. URL <https://www.R-project.org/>.
23. Lindbom L, Ribbing J, Jonsson EN. Perl-speaks-NONMEM (PsN) - A Perl module for NONMEM related programming. *Comput Methods Programs Biomed* (2004) **75**:85–94. doi:10.1016/j.cmpb.2003.11.003
24. Kagan L. Pharmacokinetic Modeling of the Subcutaneous Absorption of Therapeutic Proteins. *Drug Metab Dispos* (2014) **42**:1890–1905. doi:10.1124/DMD.114.059121

Figure legends

Figure 1: Mean and upper standard deviation of plasma concentrations over time of BIM23B065 (a, b) and BIM23B133 (c, d) after subcutaneous administration of BIM23B065 for the single ascending dose cohorts (a, c) and at day 13 of the multiple ascending dose cohorts (b, d). Circle: 0.1 mg, triangle: 0.4 mg, square: 0.8 mg, plus: 1.2 mg, crossed box: 1.5 mg, cross: 1.2 mg q.d., open circle: 0.8 mg b.i.d., open triangle: 1.0 mg b.i.d. Horizontal line at 0.10 ng/ml indicates the lower limit of quantification.

Figure 2: Structural pharmacokinetic/pharmacodynamic model including the PK of BIM23B065 and BIM23B133 and the effect of BIM23B065 on the RPP. k_a : absorption rate constant, k_{in}/k_{out} : turnover rate constants.

Figure 3: Individual model predictions versus observations (top), population model predictions versus observations (middle) and the conditional weighted residuals with interaction (CWRESI)

versus population predictions (bottom) for (a) BIM23B065, (b) BIM23B133 and the rate-pressure product of (c) placebo and (d) BIM23B065 treated subjects.

Figure 4: Mean \pm standard deviation of baseline corrected heart rate (top), systolic blood pressure (middle), and the rate-pressure product (RPP) during the first 12 hours after the first dose for placebo and single ascending dose cohorts and the final day of dosing, day 13, for the multiple ascending dose cohorts. q.d.: single daily dosing, b.i.d.: twice daily dosing at 8h and 16h intervals.

Figure 5: The rate-pressure product over time for the single ascending dose cohorts for a typical individual. Dosing clock time: 10:00. End of simulation clock time: 24:00.

ACCEPTED

Table 1: Summary of patient characteristics of the placebo and BIM23B065 treated individuals.

Demographic	Placebo (n=16)	BIM23B065 (n=47)
Age (years)	23.1 ± 4.0	23.8 ± 5.8
Weight (kg)	78.0 ± 10.3	78.2 ± 10.7
BMI (kg/m ²)	22.6 ± 2.3	23.3 ± 2.5
Height (m)	1.86 ± 0.06	1.83 ± 0.06
Lean body mass (kg)	62.4 ± 6.0	61.6 ± 6.1

BMI = body mass index, numbers given in mean ± standard deviation

Table 2: Population parameter estimates for the pharmacokinetic model of BIM23B065 (parent) and BIM23B133 (metabolite)

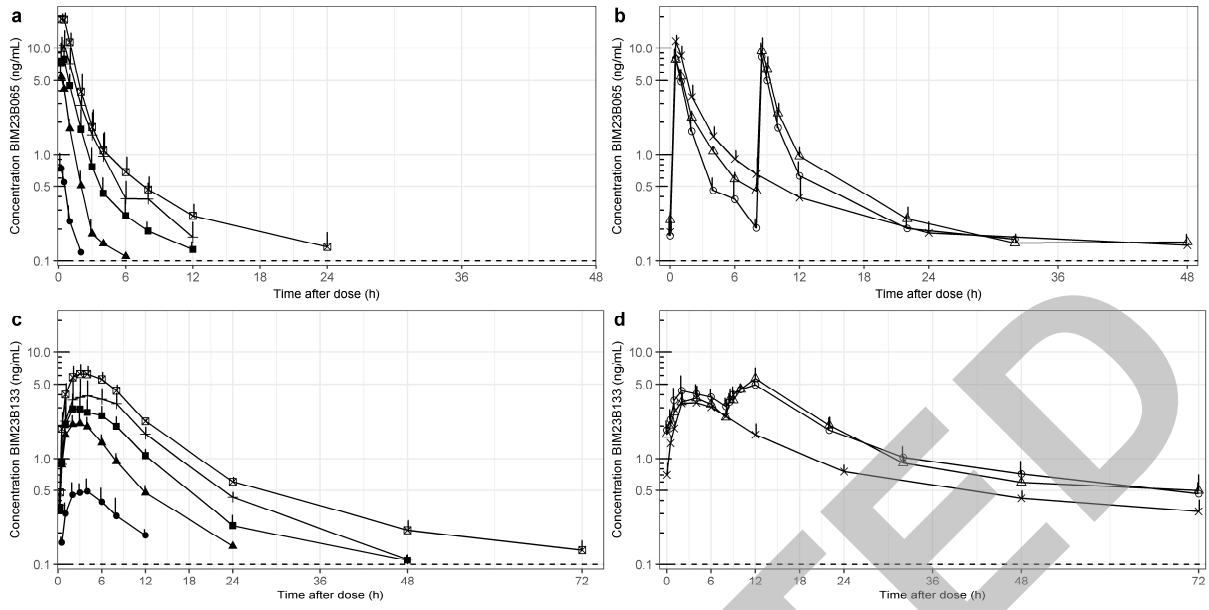
Parameter	Units	Estimate [RSE%] (CV%)	Bootstrap 95%- confidence interval
<i>Population parameters</i>			
k_a -intercept	/h	2.41 [14]	1.86 - 2.84
k_a -slope	/h/23.31 kg/m ²	-1.35 [22.4]	-1.74 - -0.85
$V_{\text{central-parent}}$	L	8.76 [40.7]	6.66 - 10.92
$V_{\text{peripheral-parent}}$	L	334 [22]	283 - 386
Q_{parent}	L/h	41.5 [11.1]	38.1 - 45.1
CL_{parent}	L/h	21.8 [45.9]	16.27 - 26.49
V_{max}	mg/h	0.0788 [22]	0.0596 - 0.1048
K_M	μg/L	0.673 [28.7]	0.44 - 1.0
KT_{linear}	/h	0.22 [6.26]	0.20 - 0.25
$KT_{\text{non-linear}}$	/h	0.332 [13.3]	0.27 - 0.41
$V_{\text{central-metabolite}}$	L	5.51 [13.7]	4.15 - 7.24
$V_{\text{peripheral-metabolite}}$	L	4230 [1.58]	1164 - 10829
$Q_{\text{metabolite}}$	L/h	11.1 [7.61]	6.36 - 16.85
$CL_{\text{S.A.D.-metabolite}}$	L/h	10.5 [7.35]	3.93 - 15.99
$CL_{\text{M.A.D.-metabolite}}$	L/h	18.5 [8.1]	12.08 - 22.88
<i>Inter-individual variability</i>			Shrinkage (%)
$\omega^2 k_a$	-	0.0579 (24.4)	8.23
$\omega^2 K_M$	-	0.351 (64.8)	14
$\omega^2 CL_{\text{parent}}$	-	0.304 (59.6)	12.1
$\omega^2 KT_{\text{non-linear}}$	-	0.585 (89.1)	17.0
$\omega^2 CL_{\text{S.A.D.-metabolite}}$	-	0.142 (39)	8.35
$\omega^2 CL_{\text{M.A.D.-metabolite}}$	-	0.0662 (26.2)	3.69
$\omega^2 V_{\text{central-metabolite}}$	-	0.346 (64.3)	27.6
<i>Residual error</i>			
$\sigma^2_{\text{Proportional}_{\text{parent}}}$	-	0.0216	12.3
$\sigma^2_{\text{Additive}_{\text{parent}}}$	-	1.69e-03	12.3
$\sigma^2_{\text{Proportional}_{\text{Metabolite}}}$	-	0.062	7.22

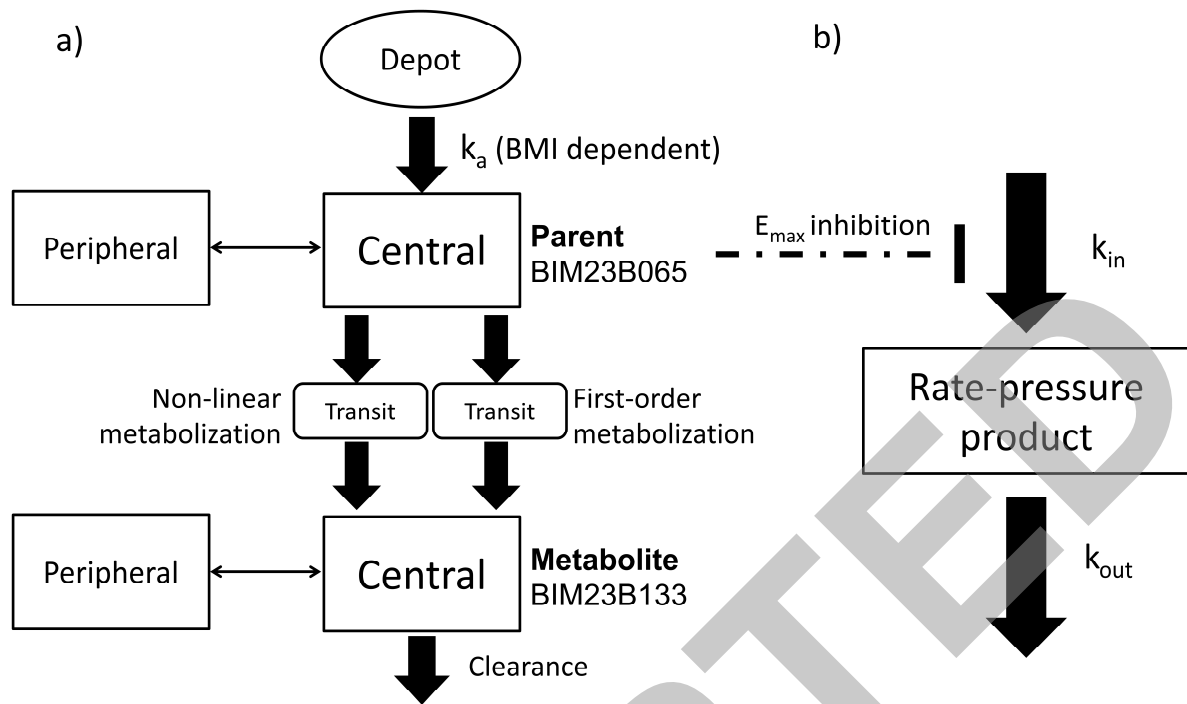
RSE = relative standard error, CV% = coefficient of variation, $k_a = k_a\text{-intercept} + k_a\text{-slope} * (\text{BMI}/23.31)$, S.A.D. = single ascending dose, M.A.D. = multiple ascending dose part.

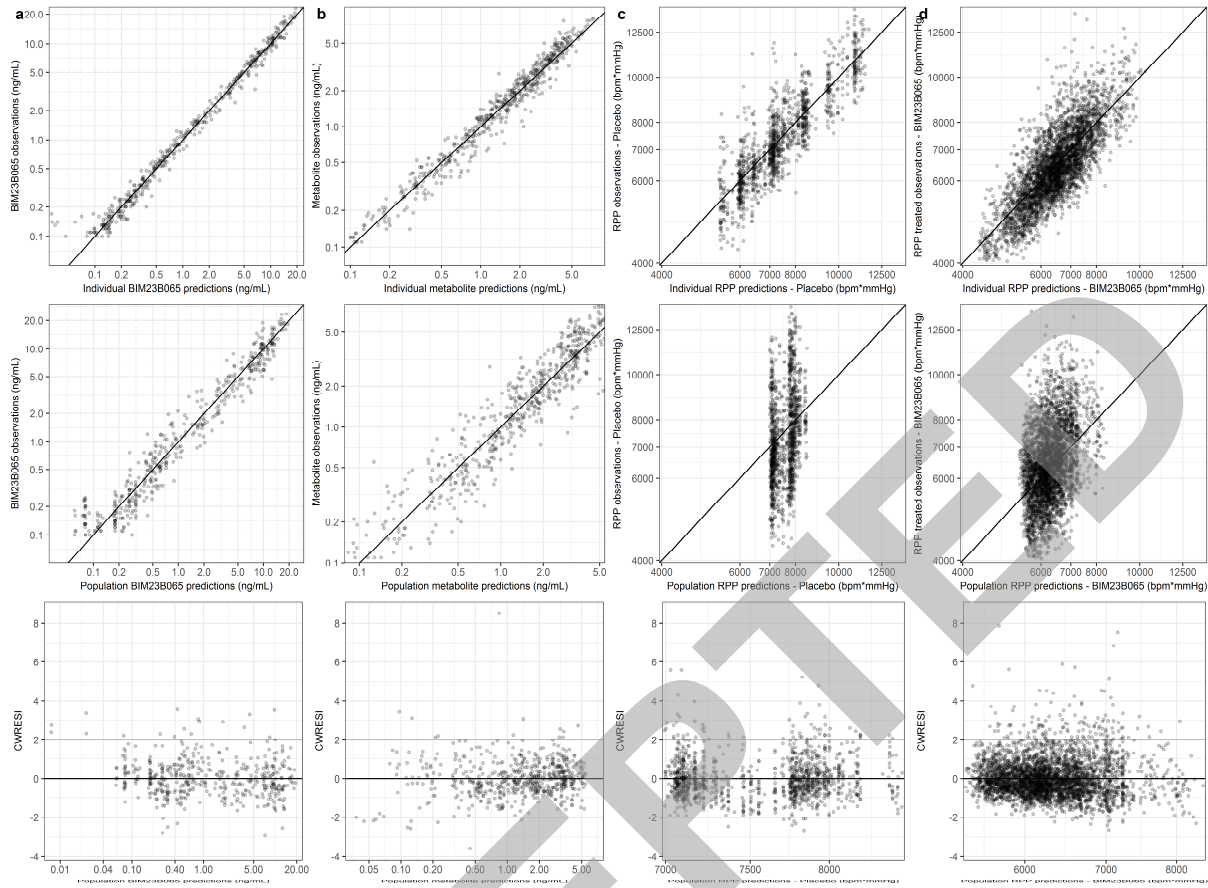
Table 3: Population parameter estimates for the pharmacodynamic model of the rate-pressure product.

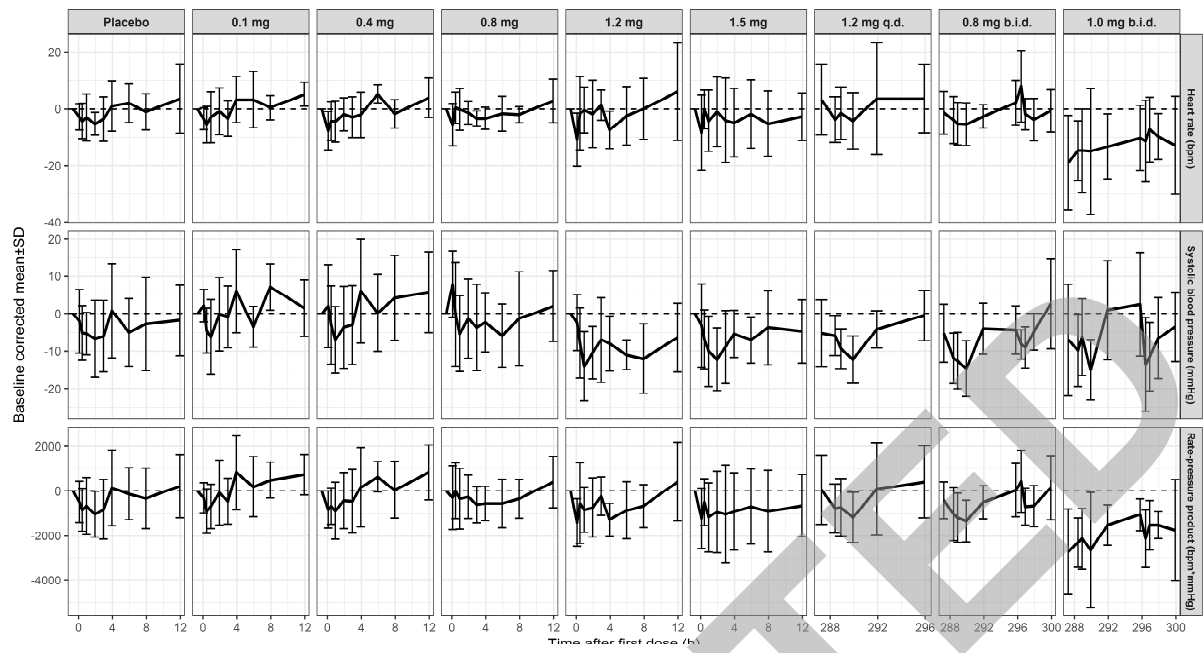
Parameter	Units	Estimate [RSE%] (CV%)	Bootstrap 95%-confidence interval
<i>Population parameters</i>			
Mesor	mmHg·bpm/h	4250 [12.1]	2194 – 7106
k_{out}	/h	0.559 [12.4]	0.286 – 0.95
Amplitude cos 24h	mmHg·bpm/h	391 [7.7]	287 – 545
Phase shift cos 24h	h	11.3 [3.43]	10.0 – 13.0
Amplitude cos 8h	mmHg·bpm/h	320 [12]	196 – 479
Phase shift cos 8h	h	1.31 [8.46]	0.83 – 1.69
<i>Drug effect parameters</i>			
E_{max}	mmHg·bpm/h	1330 [8.36]	840 – 1872
EC ₅₀ of BIM23B065	ng/mL	0.244 [12.1]	0.106 – 0.522
Tolerance slope on EC ₅₀	% increase / (mg·h/L BIM23B065)	7.07 [19.5]	1.56 – 22.87
<i>Inter-individual variability</i>			Shrinkage (%)
$\omega^2 k_{out}$	-	0.0143 (12%)	3.36
ω^2 Amplitude cos 24h	-	0.0897 (30.6%)	38.1
ω^2 Phase shift cos 24h	-	1.64 (11.3%)	34.6
ω^2 Tolerance slope	-	3.55 (581%)	17
<i>Residual error</i>			
σ^2 Additive	-	715000	1.26

Cos = cosine function, RSE = relative standard error, CV% = coefficient of variation.

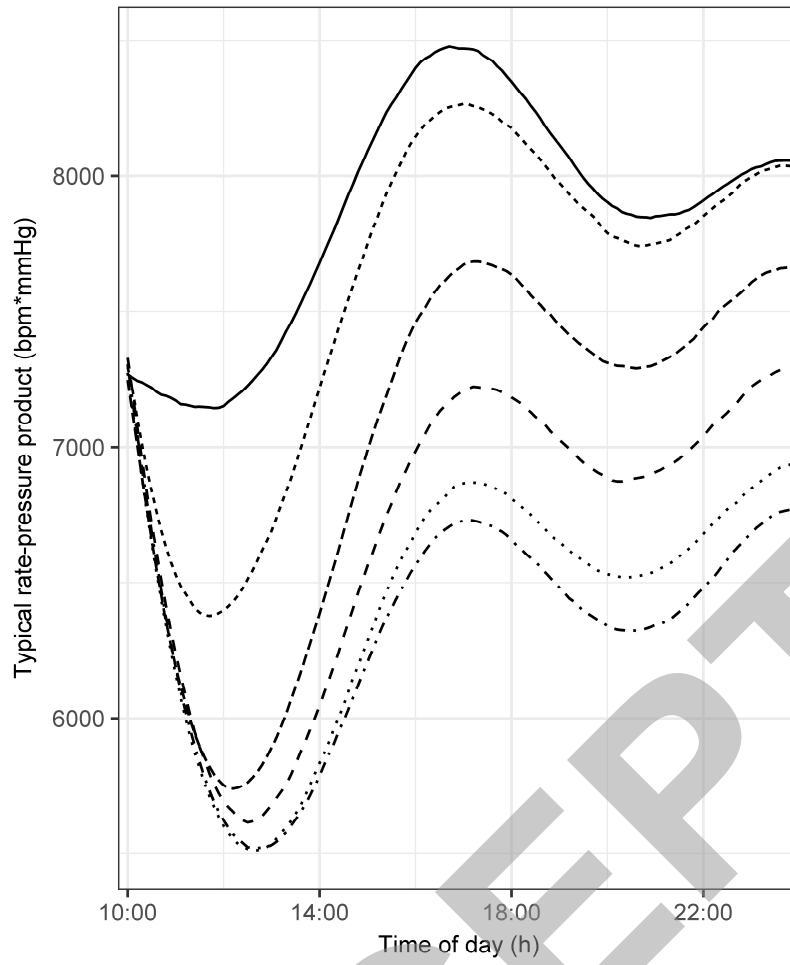








ACCEPTED



— Placebo --- 0.4 mg ··· 1.2 mg
···· 0.1 mg - - - 0.8 mg · · · 1.5 mg